 CMES, vol.53, no.2, pp.153-179, 2009

A Thermal Tomography Problem in Estimating the Unknown Interfacial Enclosure in a Multiple Region Domain with an Internal Cavity

Cheng-Hung Huang[1] **and Meng-Ting Chaing**[1]

Abstract: A three-dimensional thermal tomography problem (or inverse geometry problem) in estimating the unknown irregular shape of interfacial enclosure (or surface) for a multiple region domain with an internal cavity by using the steepest descent method (SDM) and a general purpose commercial code CFD-ACE+ is examined in the present work based on the simulated measured temperature distributions on the outer surface obtained by infrared thermography. The advantage of calling CFD-ACE+ as a subroutine in this thermal tomography problem lies in its characteristics of easily-handling the moving boundary problem considered here since it has the function of automatic grid generation. Three test cases are examined to test the validity of the present thermal tomography algorithm by using different shapes of interfacial enclosure surface, initial guesses and measurement errors. Results show that reliable estimations on the unknown geometry of the interfacial enclosure can be obtained.

Nomenclature

$f(x,y,z)$	unknown shape for irregular interfacial enclosure
J	functional defined by equation (3)
J'_x, J'_y, J'_z	gradient of functional defined by equation (18)
k	thermal conductivity
q_o	heat flux density
S_i	inner cavity surface
S_o	outer boundary surface
$T_i(x,y,z)$	estimated temperatures defined by equations (1) and (2)
$\Delta T_i(x,y,z)$	sensitivity functions defined by equations (7) and (8)
$Y_1(x,y,z)$	measured temperatures

[1] Department of Systems and Naval Mechatronic Engineering, National Cheng Kung University, Tainan, Taiwan, R.O.C.

Greeks

β	search step size defined by equation (11)
Ω	Computational domain
$\lambda_i(x,y,z)$	adjoint functions defined by equations (14) and (15)
$\delta(\bullet)$	Dirac delta function
ω	random numbeR
ε	convergence criterion
σ	standard deviation of the measurement errors

Superscript

n	iteration index

Subscripts

1	region 1
2	region 2

1 Introduction

The inverse geometry problems in the field of thermal sciences can be called as the thermal tomography problems and applied to many practical industrial and engineering applications. Generally speaking it can be classified into two categories in this research area, i.e. the shape design problems and the shape identification problems.

The feature of the thermal tomography problems is that it requires a complete regeneration of the mesh as the geometry evolves and this will lead to a tedious remeshing of the computational domain and is often classified as a highly ill-posed problem. For this reason it is necessary to use a proper numerical method or an efficient solver such that the above mentioned feature of this problem can be handled, especially for the three-dimensional applications.

The inverse geometry problems, including the shape design or shape identification problems have been solved by a variety of numerical methods [Kassab and Hsieh (1987), Hsieh, Choi and Liu (1989), Dems and Mroz (1987, 1998), Burczinski, Kane, and Balakrishna (1995), Cheng and Wu (2000), Burczynski, Beluch, Dlugosz, Kus, Nowakowski, and Orantek (2002), Divo, Kassab and Rodriguez (2004), Aoki, Amaya, Urago, and Nakayama (2005), Forth and Staroselsky (2005) and Mera, Elliott and Ingham (2006), Jeong and Kallivokas (2008), Liu, Chang and Chiang (2008)]. Huang and his co-workers have utilized the conjugate gradient method (CGM) and steepest descent method (SDM) to the inverse geometry problems and have published a series of relevant papers [Huang and Chao

(1997), Huang and Tsai (1998), Huang, Chiang and Chen (1998), Huang and Hsiung (1999), Huang and Chaing (2008)]. Recently, Huang and Chen (2008) also applied SDM to a three-dimensional inverse geometry problem in estimating the shape of an irregular internal cavity.

The same technique derived by Huang and his co-workers was adopted by Kwag, Park and Kim (2004), Chen and Yang (2009) and Chen, Yang and Lee (2009) to the shape identification problems in determining the phase front motion of ice, frost thickness and pipe fouling layer, respectively.

It should be noted that in the above references only the work by Huang and Chaing (2008), Huang and Chen (2008) and Chen, Yang and Lee (2009) are the three-dimensional problems, this implies that the three-dimensional inverse geometry problems are still very limited in the literature especially when an internal cavity exists. The three-dimensional shape identification problem using thermal tomography technique in estimating the interfacial enclosure in a multiple region domain with an internal cavity has never been examined before.

The objective of this work is to extend the algorithm of previous study by Huang and Chen (2008) to estimate the unknown three-dimensional interfacial enclosure in a multiple region domain with an internal cavity by utilizing the SDM and CFD-ACE+ code (2005). The unknown variables become x, y and z-coordinates of the interfacial enclosure and this implies that there is a huge number of unknowns in this work. The advantages of using CFD-ACE+ have been reported in the works by Huang and Chaing (2008) and Huang and Chen (2008).

The SDM is also called an iterative regularization method, this implies the regularization procedure is performed during the iterative processes and thus the determination of optimal regularization parameter is not needed. Finally the numerical experiments for this work with three different irregular interfacial enclosures will be illustrated to show the validity of using the SDM in the present three-dimensional thermal tomography problem.

2 The Direct Problem

The following three-dimensional steady-state heat conduction equation in a multiple region domain with an internal cavity is considered to illustrate the methodology for developing expressions for use to determine the shape of the unknown interfacial surface.

For the region Ω_1 the boundary condition on outer surface S_o is subjected to a known heat flux q_0. The boundary condition on inner cavity surface S_i for region Ω_2 is subjected to the prescribed temperature condition $T = T_i$. The interfacial surface is located inside the domain bounded by the inner and outer surfaces S_i and S_o,

respectively, and a perfect contact condition is applied to the interfacial enclosure $f(x,y,z)$ between Ω_1 and Ω_2, i.e. the temperature and heat flux on $f(x,y,z)$ are the same in both Ω_1 and Ω_2 domains.

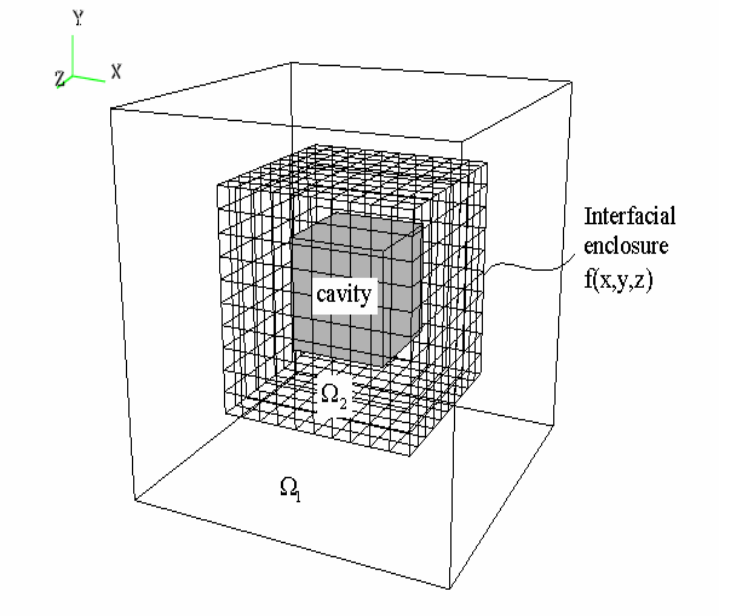

Figure 1: Geometry and coordinates.

Figure 1 shows the geometry and the coordinates for the three-dimensional physical problem considered here and the mathematical formulation of this three-dimensional heat conduction problem in a multiple region domain with the shape of interfacial surface unknown is given by the following equations:

Region Ω_1:

$$\frac{\partial^2 T_1(\Omega_1)}{\partial x^2}+\frac{\partial^2 T_1(\Omega_1)}{\partial y^2}+\frac{\partial^2 T_1(\Omega_1)}{\partial z^2}=0;\ \text{in } \Omega_1 \tag{1a}$$

$$\pm k_1\frac{\partial T_1(\Omega_1)}{\partial n}=q_0;\ \text{on outer boundary surface } S_o \tag{1b}$$

Region Ω_2:

$$\frac{\partial^2 T_2(\Omega_2)}{\partial x^2}+\frac{\partial^2 T_2(\Omega_2)}{\partial y^2}+\frac{\partial^2 T_2(\Omega_2)}{\partial z^2}=0;\ \text{in } \Omega_2 \tag{1c}$$

$$T = T_i; \text{ on inner cavity surface } S_i \tag{1d}$$

Interfacial conditions for regions Ω_1 and Ω_2 on $f(x,y,z)$:

$$T_1(\Omega_1) = T_2(\Omega_2); \text{ on the unknown interface } f(x,y,z) \tag{2a}$$

$$k_1 \frac{\partial T_1(\Omega_1)}{\partial n} = k_2 \frac{\partial T_2(\Omega_2)}{\partial n}; \text{ on the unknown interface } f(x,y,z) \tag{2b}$$

here subscripts 1 and 2 denote two different domains with thermal conductivities k_1 and k_2, respectively. The above direct problem can be solved by the commercial code CFD-ACE+ for the reason that it has the ability to auto mesh the grid systems.

The direct problem considered here is concerned with the determination of the domain temperature distributions when the interfacial geometry of $f(x,y,z)$, thermal properties and the boundary conditions are given and known.

3 The Thermal Tomography Problem

For the thermal tomography problem, the geometry of interfacial enclosure $f(x,y,z)$ is regarded as being unknown, but everything else in direct problem, i.e. equations (1) and (2), are known. In additions, temperature readings taken by the imaginary infrared scanner on the outer surface S_o are considered available. It should be noted that the geometry of interfacial enclosure $f(x,y,z)$ is located inside the domain bounded by the inner and outer surfaces S_i and S_o, respectively,

Referring to figure 1, let the temperature reading on the outer surface S_o be denoted by $Y_{1,m}(S_o) \equiv Y_{1,m}(x_m, y_m, z_m)$, m = 1 to M, where M represents the total number of measured temperature extracting points. It is noted that the measured temperature $Y_{1,m}(S_o)$ contain measurement errors. This thermal tomography problem can be stated as follow: by utilizing the above mentioned measured temperature data $Y_{1,m}(S_o)$, estimates the unknown geometry of the interfacial enclosure $f(x,y,z)$.

The solution of the present thermal tomography problem is to be obtained in such a way that the following functional is minimized:

$$J[f(x,y,z)] = \sum_{m=1}^{M} [T_{1,m}(\mathrm{S}_o) - Y_{1,m}(S_o)]^2 \tag{3}$$

where $T_{1,m}$ is the estimated or computed temperature at the measurement locations(x_m, y_m, z_m) on S_o. These quantities are determined from the solution of the direct problem given previously by using an estimated $f(x,y,z)$ for the exact $f(x,y,z)$. In our algorithm the number of interfacial surface grid points must be equal to or less than the number of surface temperature measurements to obtain accurate estimations.

4 The Steepest Descent Method for Minimization

The steepest descent method (SDM) is similar to but simpler than the conjugate gradient method (CGM) [Alifanov (1994)] since the calculations of the conjugate coefficient and direction of descent are not needed. It is found that the SDM achieves our goal in this thermal tomography study and converges fast. The following iterative process based on the SDM is now used for the estimation of the unknown geometry of interfacial enclosure $f(x,y,z)$ by minimizing the functional $J[f(x,y,z)]$.

$$f^{n+1}(x^{n+1},y^{n+1},^{n+1}) = f^n(x^n,y^n,^n) - \beta^n J'^n \tag{4a}$$

where

$$J'^n(x,y,z) = J'^n_x\vec{i} + J'^n_y\vec{j} + J'^n_z\vec{k} \tag{4b}$$

or more explicitly

$$x^{n+1} = x^n - \beta^n J'^n_x(x,y,) \tag{5a}$$

$$y^{n+1} = y^n - \beta^n J'^n_y(x,y,) \tag{5b}$$

$$z^{n+1} = z^n - \beta^n J'^n_z(x,y,) \tag{5c}$$

and

$$\hat{f}^{n+1}(x,y) \equiv f(\hat{x}^{n+1},\hat{y}^{n+1}) \tag{6}$$

Here β^n is the search step size in going from iteration n to iteration n+1, $J'^n(x,y,z)$ is the gradient in the outward normal direction while $J'^n_x(x,y,z)$, $J'^n_y(x,y,z)$ and $J'^n_z(x,y,z)$ are the gradients in x, y and z direction, respectively.

To perform the iterations according to equation (4), the step size β^n and the gradients of the functional $J'^n_x(x,y,z)$, $J'^n_y(x,y,z)$ and $J'^n_z(x,y,z)$ must be calculated. In order to develop expressions for the determination of the above quantities, a "sensitivity problem" and an "adjoint problem" are constructed as described below.

5 Sensitivity Problem and Search Step Size

The sensitivity problem is obtained from the original direct problem defined by equations (1) and (2) in the following manner: It is assumed that when $f(x,y,z)$

undergoes a variation $\Delta f(x,y,z)$, T_1 and T_2 are perturbed by ΔT_1 and ΔT_2. By replacing f by f+Δf, T_1 by $T_1+\Delta T_1$ and T_2 by $T_2+\Delta T_2$ in the direct problem, subtracting the resulting expressions from the direct problem and neglecting the second-order terms, the following sensitivity problem for the sensitivity functions ΔT_1 and ΔT_2 can be obtained.

Region Ω_1:

$$\frac{\partial^2 \Delta T_1(\Omega_1)}{\partial x^2}+\frac{\partial^2 \Delta T_1(\Omega_1)}{\partial y^2}+\frac{\partial^2 \Delta T_1(\Omega_1)}{\partial z^2}=0;\ \text{in } \Omega_1 \tag{7a}$$

$$\frac{\partial \Delta T_1(\Omega_1)}{\partial n}=0;\ \text{on outer boundary surface } S_o \tag{7b}$$

Region Ω_2:

$$\frac{\partial^2 \Delta T_2(\Omega_2)}{\partial x^2}+\frac{\partial^2 \Delta T_2(\Omega_2)}{\partial y^2}+\frac{\partial^2 \Delta T_2(\Omega_2)}{\partial z^2}=0;\ \text{in } \Omega_2 \tag{7c}$$

$$\Delta T_2=0;\ \text{on inner cavity surface } S_i \tag{7d}$$

Interfacial conditions for regions Ω_1 and Ω_2 can be obtained as:

$$\Delta T_1(\Omega_1)=T_1(\Omega_1;f+\Delta f)-T_1(\Omega_1;f)\cong \Delta f\frac{\partial T_1(\Omega_1)}{\partial n};\ \text{on } f(x,y,z) \tag{8a}$$

$$\Delta T_2(\Omega_2)=T_2(\Omega_2;f+\Delta f)-T_2(\Omega_2;f)\cong \Delta f\frac{\partial T_2(\Omega_2)}{\partial n};\ \text{on } f(x,y,z) \tag{8b}$$

It should be noted that the sensitivity problems are now de-coupled as two independent problems since the interfacial conditions become independent to each other now, this differs from our previous relevant works. The above two sensitivity problems can be solved by the commercial code CFD-ACE+ separately.

Based on equations (2) and (8), the following interfacial conditions can also be obtained

$$\Delta T_1(\Omega_1)=\frac{k_2}{k_1}\Delta T_2(\Omega_2);\ \text{on } f(x,y,z) \tag{9a}$$

$$k_1\frac{\partial \Delta T_1(\Omega_1)}{\partial n}=k_2\frac{\partial \Delta T_2(\Omega_2)}{\partial n};\ \text{on } f(x,y,z) \tag{9b}$$

The above two equations are needed in deriving the interfacial conditions for the adjoint problem. The functional $J(f^{n+1})$ for iteration n+1 is obtained by rewriting equation (3) as

$$J[f^{n+1}]=\sum_{m=1}^{M}\left[T_{1,m}(f^n-\beta^n J'^n)-Y_{1,m}\right]^2 \tag{10a}$$

where we have replaced f^{n+1} by the expression given by equation (4a). If temperature $T_{1,m}(f^n - \beta^n J'^n)$ is linearized by a Taylor expansion, equation (10a) takes the form

$$J(f^{n+1}) = \sum_{m=1}^{M} [T_{1,m}(f^n) - \beta^n \Delta T_{1,m}(J'^n) - Y_{1,m}]^2 \tag{10b}$$

where $T_{1,m}(f^n)$ is the solution of the direct problem at (x_m, y_m, z_m) by using estimate $f(x,y,z)$ for exact $f(x,y,z)$. The sensitivity function $\Delta T_{1,m}(J'^n)$ is taken as the solution of problem (7) at the measured positions (x_m, y_m, z_m) by letting $\Delta f = J'^n$. The search step size β^n is determined by minimizing the functional given by equation (10b) with respect to β^n. The following expression results:

$$\beta^n = \frac{\sum_{m=1}^{M} (T_{1,m} - Y_{1,m}) \Delta T_{1,m}}{\sum_{m=1}^{M} (\Delta T_{1,m})^2} \tag{11}$$

6 Adjoint Problem and Gradient Equation

To obtain the adjoint problem, equations (1a) and (1c) are multiplied by the Lagrange multipliers (or adjoint functions) $\lambda_1(x,y,z)$ and $\lambda_2(x,y,z)$, respectively and the resulting expression is integrated over the correspondent space domain. The result is then added to the right hand side of equation (3) to yield the following expression for the functional $J[f(x,y,z)]$:

$$J[f(x,y,)] = \int_{S_o} [T_1 - Y_1]^2 \delta(x - x_m)\delta(y - y_m)\delta(z - z_m) dS_o + \int_{\Omega_1} \lambda_1 \left\{ \frac{\partial^2 T_1}{\partial x^2} + \frac{\partial^2 T_1}{\partial y^2} + \frac{\partial^2 T_1}{\partial z^2} \right\} d\Omega_1 + \int_{\Omega_2} \lambda_2 \left\{ \frac{\partial^2 T_2}{\partial x^2} + \frac{\partial^2 T_2}{\partial y^2} + \frac{\partial^2 T_2}{\partial z^2} \right\} d\Omega_2 \tag{12}$$

The variation ΔJ is obtained by perturbing f by $\Delta f, T_1$ by ΔT_1 and T_2 by ΔT_2 in equation (12), subtracting the resulting expression from the original equation (12) and neglecting the second-order terms. This yields:

$$\Delta J = \int_{S_o} 2(T_1 - Y_1)\Delta T_1 \delta(x - x_m)\delta(y - y_m)\delta(z - z_m) dS_o + \int_{\Omega_1} \lambda_1 \left\{ \frac{\partial^2 \Delta T_1}{\partial x^2} + \frac{\partial^2 \Delta T_1}{\partial y^2} + + \frac{\partial^2 \Delta T_1}{\partial z^2} \right\} d\Omega_1 +$$

In equation (13), the domain integral term is reformulated based on Green's second identity; the boundary conditions of the sensitivity problems are utilized and then

ΔJ is allowed to go to zero. The vanishing of the integrands containing ΔT_1 and ΔT_2 leads to the following adjoint problems for determining the values of $\lambda_x(\Omega_1)$ and $\lambda_y(\Omega_2)$: Region Ω_1:

$$\frac{\partial^2\lambda_1(\Omega_1)}{\partial x^2}+\frac{\partial^2\lambda_1(\Omega_1)}{\partial y^2}+\frac{\partial^2\lambda_1(\Omega_1)}{\partial z^2}=0 \text{ in } \Omega_1 \tag{14a}$$

$$\frac{\partial\lambda_1}{\partial n}=2(T_1-Y_1)\delta(x-x_m)\delta(y-y_m)\delta(z-z_m); \text{ on inner boundary surface } S_o \tag{14b}$$

Region Ω_2:

$$\frac{\partial^2\lambda_2(\Omega_2)}{\partial x^2}+\frac{\partial^2\lambda_2(\Omega_2)}{\partial y^2}+\frac{\partial^2\lambda_2(\Omega_2)}{\partial z^2}=0; \text{ in } \Omega_2 \tag{14c}$$

$$\lambda_2=0; \text{ on inner cavity surface } S_i \tag{14d}$$

Interfacial conditions for regions Ω_1 and Ω_2:

$$\lambda_1(\Omega_1)=\frac{k_1}{k_2}\lambda_2(\Omega_2) \quad ; \text{ on } f(x,y,z) \tag{15a}$$

$$k_2\frac{\partial\lambda_1(\Omega_1)}{\partial n}=k_1\frac{\partial\lambda_2(\Omega_2)}{\partial n}; \text{ on } f(x,y,z) \tag{15b}$$

The commercial code CFD-ACE+ is utilized to solve the above adjoint problem. Finally, the following integral term is left

$$\Delta J=\int_f -\left[\frac{\partial\lambda_1}{\partial n}\frac{\partial T_1}{\partial n}\right]\Delta f(x,y,z)df \tag{16a}$$

From definition [Alifanov (1994)], the functional increment can be presented as

$$\Delta J=\int_f J'(x,y,z)\Delta f(x,y,z)df \tag{16b}$$

A comparison of equations (16a) and (16b) leads to the following expression for the gradient of functional $J'(x,y,z)$ of the functional $J[f(x,y,z)]$:

$$J'(x,y,z)=-\frac{\partial\lambda_1}{\partial n}\frac{\partial T_1}{\partial n}\bigg|_f=-(J'_x|_f)\vec{i}-(J'_y|_f)\vec{j}-(J'_z|_f)\vec{k} \tag{17}$$

Finally the following gradient equations can be obtained

$$J'_x(x,y,z) = -\frac{\partial \lambda_1}{\partial n}\frac{\partial T_1}{\partial n}\vec{n}_i \tag{18a}$$

$$J'_y(x,y,z) = -\frac{\partial \lambda_1}{\partial n}\frac{\partial T_1}{\partial n}\vec{n}_j \tag{18b}$$

$$J'_z(x,y,z) = -\frac{\partial \lambda_1}{\partial n}\frac{\partial T_1}{\partial n}\vec{n}_k \tag{18c}$$

The calculation of gradient equations is the most important part of the SDM since it plays a significant role of the thermal tomography calculations. Besides, from Equation (5) we know that the new shape is a function of the gradients, and from Equation (18) it shows that the gradient is a function of normal outward vector in x, y and z directions. This implies that before new interfacial enclosure can be estimated, the normal outward vector $\vec{n}$ must be calculated.

7 Stopping Criterion

If the problem contains no measurement errors, the traditional check condition specified as follow can be used as the stopping criteria

$$J\left[f^{n+1}(x,y,z)\right] < \varepsilon \tag{19a}$$

where ε is a small specified number and a monotonic convergence can be obtained with SDM. However, the observed temperature data may contain measurement errors. Therefore, it is not expected that the functional equation (4) to be equal to zero at the final iteration step. Following the experience of the author [Alifanov (1994)], the discrepancy principle is used as the stopping criterion, i.e. it is assumed that the temperature residuals may be approximated by

$$T_m - Y_m \approx \sigma \tag{19b}$$

where σ is the standard deviation of the measurement errors, which is assumed to be a constant. Substituting equation (19b) into equation (4), the following expression is obtained for ε:

$$\varepsilon = M\sigma^2 \tag{19c}$$

For this reason the stopping criterion is given by equation (19a) with ε determined from equation (19c).

8 Computational Procedure

The computational procedure of the interfacial surface estimation for this thermal tomography problem using the SDM can be summarized as follows:

Suppose $f^n(x,y,z)$ is available at iteration n.

Step 1. Solve the direct problem given by equations (1) to (2) for $T_i(x,y,z)$.

Step 2. Examine the stopping criterion given by equation (19a) with ε given by equation (19c). Continue if not satisfied.

Step 3. Solve the adjoint problem given by equations (14) and (15) for $\lambda_i(x,y,z)$.

Step 4. Compute the gradients of the functional J'_x, J'_y and J'_z from equations (18a), (18b) and (18c), respectively.

Step 5. Set $\Delta f(x,y,z) = J'^n(x,y,z)$, and solve the sensitivity problem given by equations (7) and (8) for $\Delta T_i(x,y,z)$.

Step 6. Compute the search step size β^n from equation (11).

Step 7. Compute the new estimation for $f^{n+1}(x,y,z)$ from equation (4) and return to step 1.

9 Results and Discussions

To examine the validity of the present shape identification problem using thermal tomography technique in estimating the irregular shape for interfacial enclosure from the knowledge of the simulated temperature recordings taken by the imaginary infrared scanners on the outer surface S_o, three specific examples are considered where the shapes of exact and guessed interfacial enclosures are varied.

The geometry of the outer boundary and inner cavity for all the examples considered here are both taken as a cube with length equal to 10 cm and 3 cm, respectively, with the center located at (5,5,5) cm. The thermal conductivities for regions Ω_1 and Ω_2 are taken as k_1 = 48 W/m-K (Steel-AISI-1020) and k_2 = 210 W/m-K (Aluminum). The heat flux is taken q_o = -15000 W/m^2 and the boundary temperature for inner cavity surface is taken as $T_i = 200^o$C.

The objective of this work is to show the accuracy of the present approach in estimating the shape of interfacial enclosure $f(x,y,z)$, with no a priori information on the functional form of the unknown shape, it is classified as the function estimation.

In order to compare the results for situations involving random measurement errors, the normally distributed uncorrelated errors with zero mean and constant standard deviation were assumed. The simulated inexact measurement data $\mathbf{Y}$ can be expressed as

$$\mathbf{Y}_1 = \mathbf{Y}_{1,dir} + \omega\sigma \tag{20}$$

where $\mathbf{Y}_{1,dir}$ is the solution of the direct problem with an exact $f(x,y,z)$; σ is the standard deviation of the measurement error; and ω is a random variable that generated by subroutine DRNNOR of the IMSL (1987) and will be within -2.576 to 2.576 for a 99% confidence bounds.

One of the advantages of using the SDM is that it does not require a very accurate initial guess of the unknown quantities; this can be verified in the following numerical test cases. To examine the effects of different shapes of initial guesses of the interfacial enclosure to the final estimations, two different shapes of initial guesses are used in this work. The followings define these two types of initial guesses:

Type A: A cube with length equal to 5 cm and its center located at (5,5,5) cm.

Type B: A cube with length equal to 4 cm and its center located at (5,5,5) cm.

the plots for these two initial guesses of the interfacial enclosure are shown in Figures 2(a) and 2(b), respectively.

Three numerical experiments in estimating the shape of interfacial enclosure $f(x,y,z)$ by using the SDM are presented below.

Numerical test case 1:

The unknown configuration of the exact interfacial enclosure is assumed to be a cube with the center located at (5,5,5) cm and length equal to 6 cm and is shown in Figure 3(a). The number of grids used for external, interfacial enclosure and internal domains are all $11\times11\times6$, which implies that on each external, interfacial enclosure and internal surface has 121 grid points. After deducting the overlapped grid points, there are totally of 602 grid points on the interfacial enclosure surface or (602×3) = 1806 unknown parameters of x- , y- and z-coordinates in the present case. The number of the discreted points for the exact interfacial enclosure is identical to that for the estimated interfacial enclosure in the present study.

First, when assuming exact measurements, i.e. σ = 0.0, and using type A initial guess. By choosing ε = 0.5, after 42 iterations the estimation can be obtained and the estimated shape of interfacial enclosure by using the SDM is shown in Figure 3(b). The measured and estimated temperatures for this case are presented

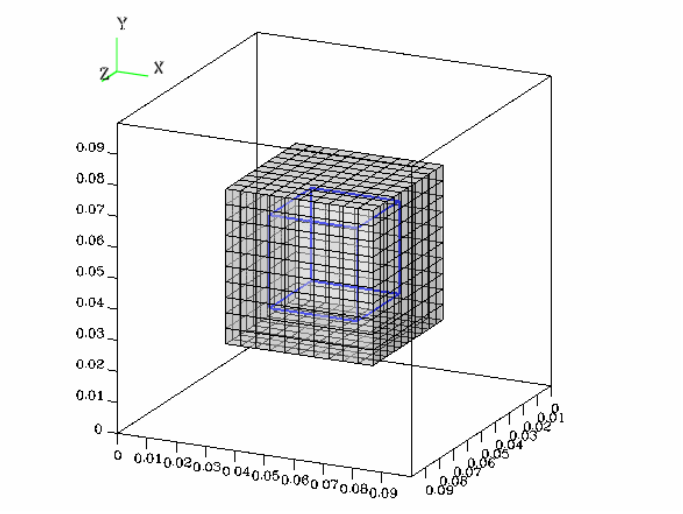

(a)

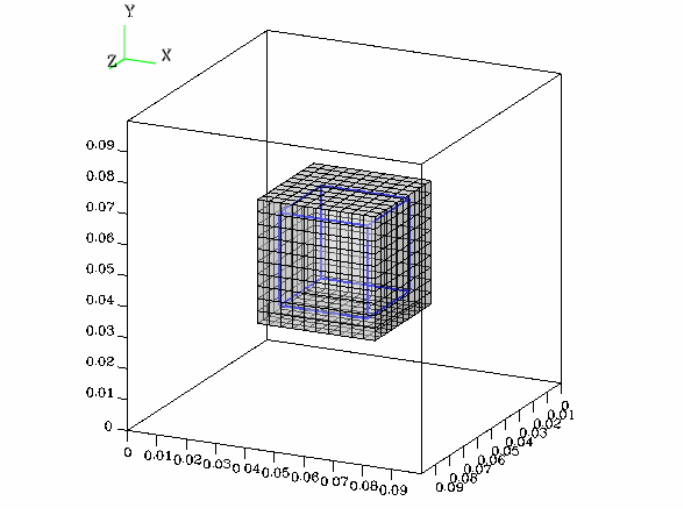

(b)

Figure 2: The (a) type A and (b) type B initial guesses for the shape of interfacial enclosure in the present study.

in Figures 4(a) and 4(b), respectively. The CPU time on Intel®Pentium D CPU 2.8 GHz PC used in the present computations is about 133 minutes.

The average relative error for the measured and estimated temperatures is calcu-

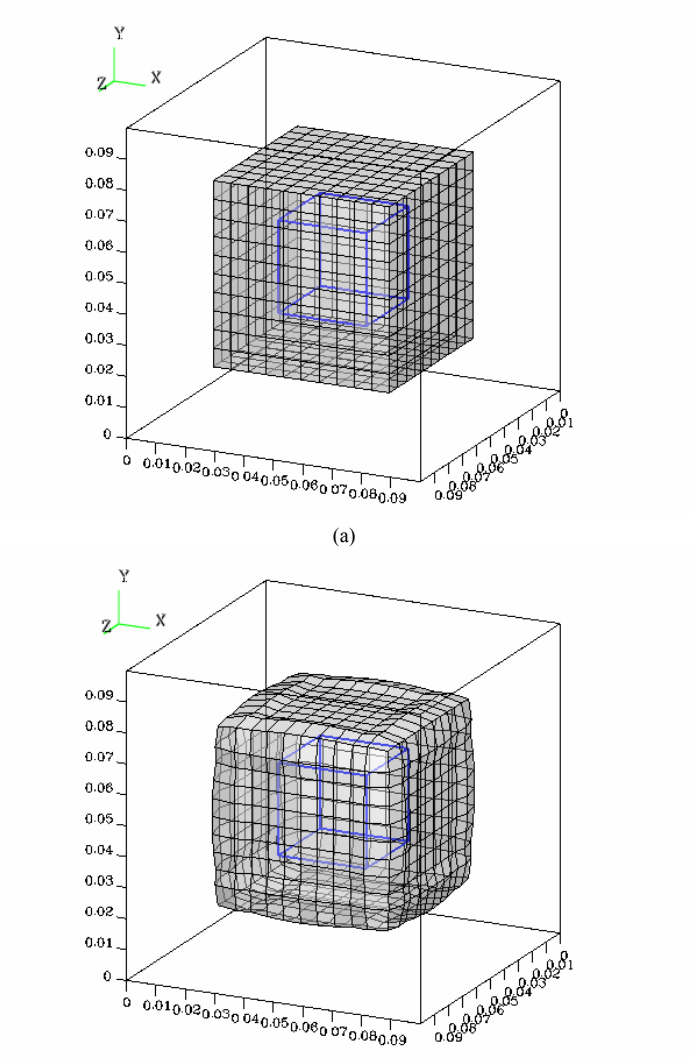

Figure 3: The (a) exact and (b) estimated interfacial enclosures using type A initial guess and $\sigma = 0.0$ in case 1.

lated as ERR = 0.005 %, where the average relative error ERR is defined as

$$\mathrm{ERR} = \sum_{m=1}^{M} \left| \frac{T(x_m, y_m, zm) - Y(x_m, y_m, zm)}{Y(x_m, y_m, zm)} \right| \div \mathrm{M} \times 100\% \tag{21}$$

here M = 602 represents the total number of measurements. It can be seen from the above figures and relative average error that the present thermal tomography scheme obtained good estimation for $f(x,y,z)$ since the shape of interfacial enclosure can still be reconstructed without assuming any extra conditions.

Next, it would be of interest to examine what will be happened when different initial guess is considered. The computational conditions are the same as the previous case except that type B initial guess is now chosen.

By choosing $\varepsilon = 2$ and $\sigma = 0.0$, after 34 iterations the estimated shape of interfacial enclosure is shown in Figure 5(a). The estimated temperatures for this case are presented in Figure 5(b). The relative average error ERR is calculated as ERR = 0.009 % and CPU time is 107 minutes. Again, it can be seen from these Figures and data that this algorithm obtained good estimation of $f(x,y,z)$, even though the initial guess is different.

Finally, the influence of the measurement errors on the thermal tomography problems needs be discussed. First, the measurement error for the simulated temperatures measured by imaginary infrared scanner on outer surface S_o is taken as σ = 0.405 (about 3 % of the largest temperature difference on S_o). The estimations for $f(x,y,z)$ can be obtained after only 15 iterations and plotted in Figures 6(a). The relative average error ERR1 is calculated as ERR = 0.066 %. The measurement error for the temperatures is then increased to $\sigma = 0.675$ (about 5 % of the largest temperature difference on S_o). After only 13 iterations the estimated $f(x,y,z)$ are obtained and illustrated in Figures 6(b) and ERR is calculated as 0.11 %.

Table 1: Numerical results for all the test cases considered in this study

Results Test cases	σ	ε	Number of iteration	CPU time (minutes)	ERR%
Numerical test case 1	0	0.5	42	133	0.005
	0.405	99	15	48	0.066
	0.675	274	13	41	0.11
Numerical test case 2	0	3	163	532	0.011
	0.504	153	20	65	0.081
	0.84	425	13	42	0.135
Numerical test case 3	0	4	173	656	0.011
	0.405	99	67	276	0.065
	0.675	274	28	110	0.109

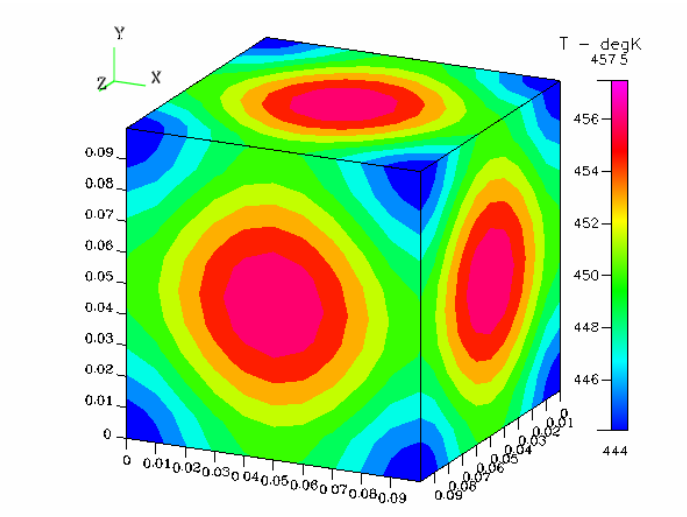

(a)

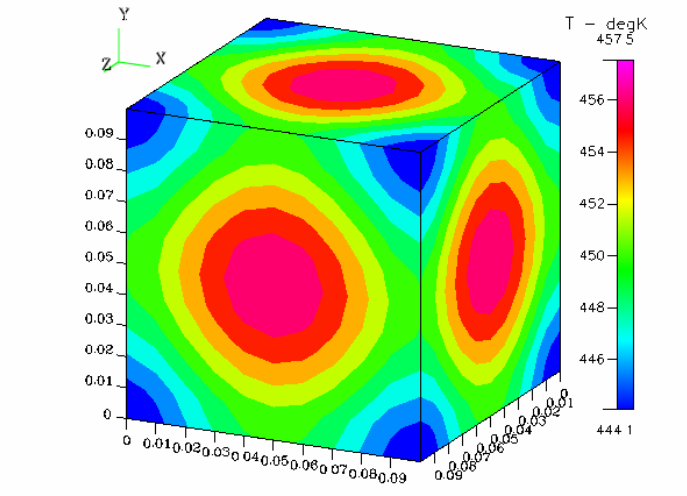

(b)

Figure 4: The (a) measured and (b) estimated surface temperatures on S_o using σ = 0.0 in case 1.

All the numerical results in test case 1 are summarized in Table 1. From Figures 3 to 6 we have learned that as the measurement errors are increased the accuracy of the estimated shape for the interfacial enclosure is decreased, however, they are still reliable. It is thus concluded that the present technique provides confidence

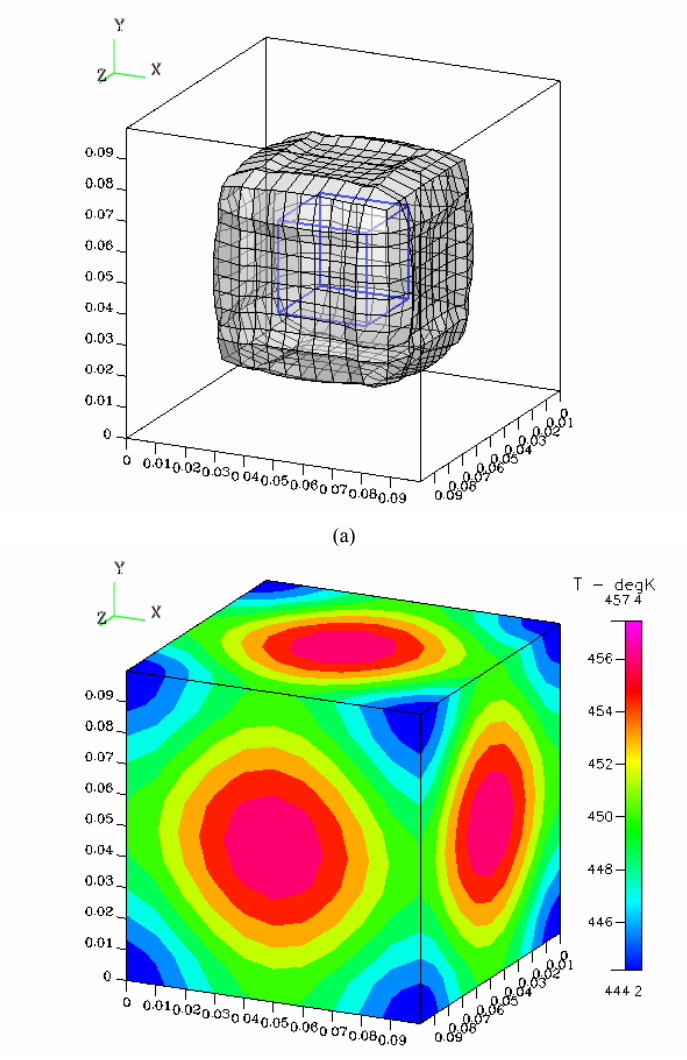

Figure 5: The (a) estimated interfacial enclosure using type B initial guess and (b) estimated surface temperatures on S_o using $\sigma = 0.0$ in case 1.

estimation.

Numerical test case 2:

In order to show the ability in handling more irregular shape for the interfacial

enclosure, in the second test case an exact interfacial enclosure as shown in Figure 7(a) is considered. The computational conditions are the same as used in numerical test case 1 and type A initial guess for the interfacial enclosure is used.

When assuming exact measurements $\sigma = 0.0$, and $\varepsilon = 3.0$, after 163 iterations, the estimated shape of the interfacial enclosure by using SDM is shown in Figure 7(b). The measured and estimated temperatures for this case are presented in Figures 8(a) and 8(b), respectively. The CPU time on Intel®Pentium D CPU 2.8 GHz PC used in the present computations is about 532 minutes.

The average relative error for the measured and estimated temperatures is calculated as ERR = 0.011 %. It is clear from the above figures and ERR that good estimation for $f(x,y,z)$ can be obtained by the present thermal tomography scheme.

Finally, let us examine the influence of the measurement errors on the thermal tomography problems. First, the measurement error for the simulated temperatures measured by imaginary infrared scanner on outer surface S_o is taken as $\sigma = 0.504$ (about 3 % of the largest temperature difference on S_o), then it is increased to $\sigma = 0.84$ (about 5 % of the largest temperature difference on S_o). The estimations for $f(x,y,z)$ can be obtained after 20 and 13 iterations, respectively and the results for the estimated interfacial enclosure are plotted in Figures 9(a) and 9(b), respectively. The relative average error for $\sigma = 0.504$ are calculated as ERR = 0.081 % and for $\sigma = 0.84$ is calculated as ERR = 0.135 %. The CPU time for both cases is about 79 and 48 minutes, respectively. The numerical results in test case 2 are summarized in Table 1. Again, the present technique provides confidence estimation.

Numerical test case 3:

To test the ability of this algorithm, in the third test case we considered another irregular shape as the exact interfacial enclosure which is shown in Figure 10(a). It can be seen from Figure 10(a) that the interfacial enclosure becomes more irregular and this makes the estimation more difficult. Type A initial guess is used in test case 3 and the computational conditions are the same as used in numerical test case 1.

When assuming exact measurements $\sigma = 0.0$ and $\varepsilon = 4.0$, and after 173 iterations, the estimated shape of the irregular by using SDM is shown in Figure 10(b). The measured and estimated temperatures for this case are presented in Figures 11(a) and 11(b), respectively. The CPU time in the present computations is about 656 minutes.

The average relative error for the measured and estimated temperatures is calculated as ERR = 0.011 %. It is clear from the above figures and ERR that good estimation for $f(x,y,z)$ can be obtained by the present thermal tomography scheme.

Finally, the measurement error for the simulated temperatures measured by imag-

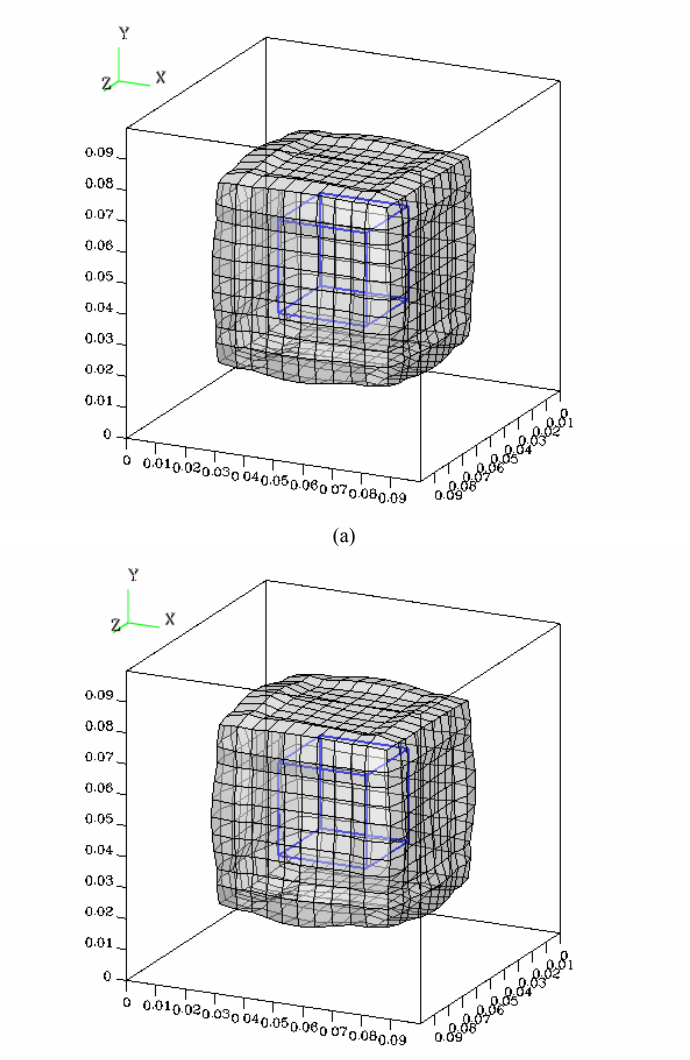

Figure 6: The estimated interfacial enclosures using (a) σ = 0.405 and (b) σ = 0.675 and type A initial guess in case 1.

inary infrared scanner on outer surface S_o is taken as σ = 0.405 (about 3 % of the largest temperature difference on S_o). The estimations for $f(x,y,z)$ can be obtained after 67 iterations and the results for the estimated cavities are plotted in Figure 12(a). The relative average error is calculated as ERR = 0.065 % and the CPU time

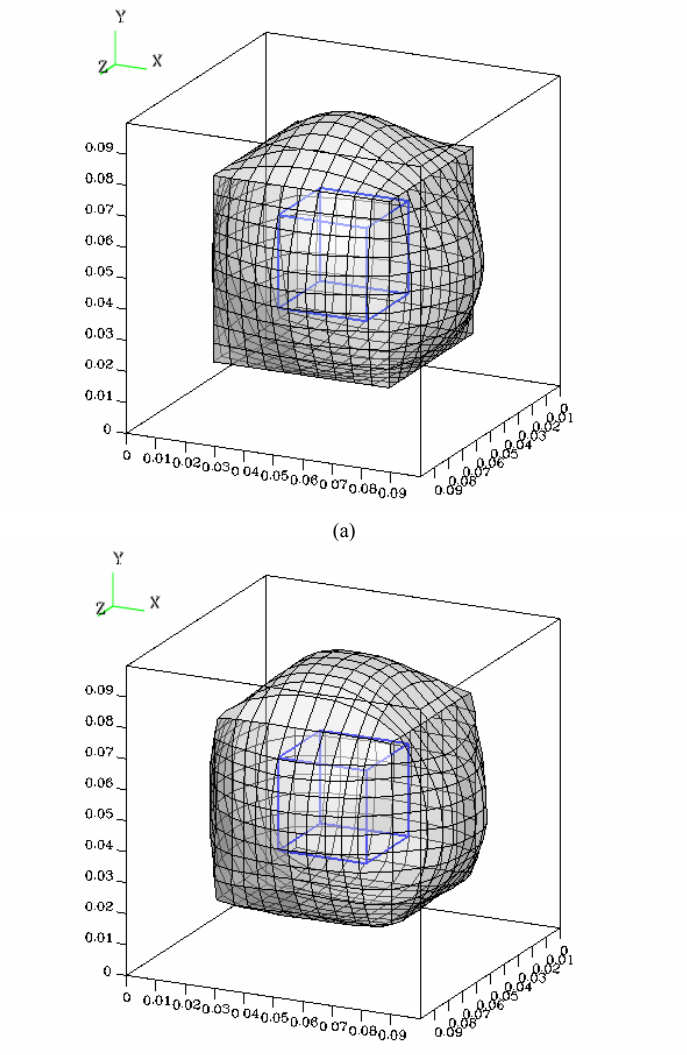

Figure 7: The (a) exact and (b) estimated interfacial enclosures using type A initial guess and $\sigma = 0.0$ in case 2.

in the present computation is about 276 minutes.

Next, the measurement error is increased to $\sigma = 0.675$ (about 5 % of the largest temperature difference on S_o). The estimation for the interfacial enclosure is obtained after 28 iterations and the results for the estimated interfacial enclosure are

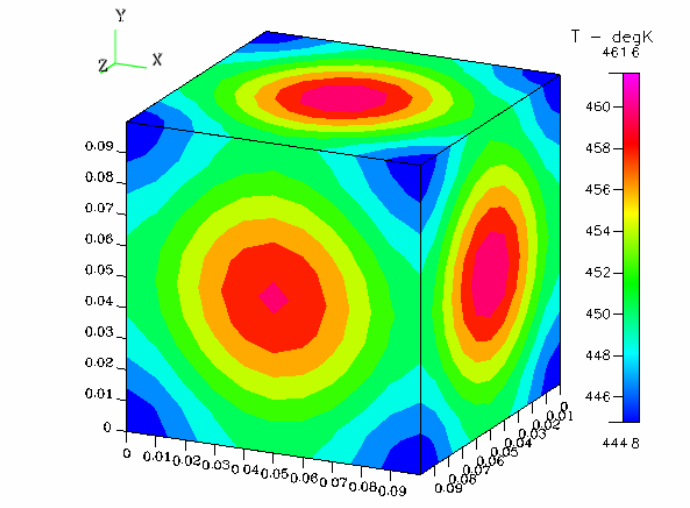

(a)

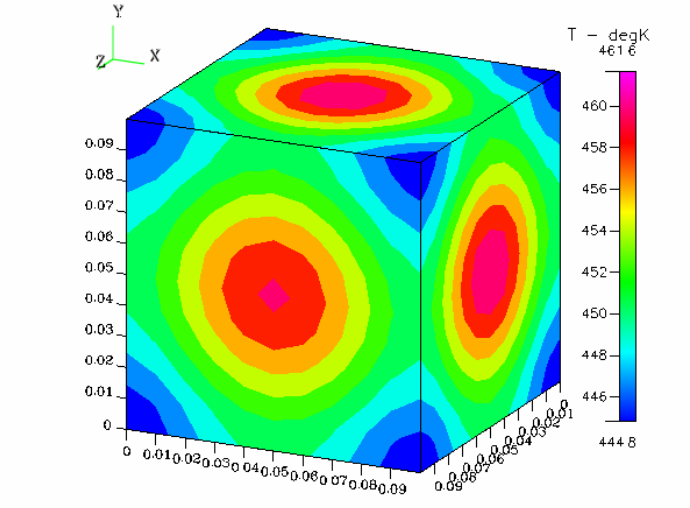

(b)

Figure 8: The (a) measured and (b) estimated surface temperatures on S_o using σ = 0.0 in case 2.

shown in Figure 12(b). The relative average error is obtained as ERR1 = 0.109 % and the CPU time in the present computation is about 110 minutes. The numerical results in this test case are summarized in Table 1.

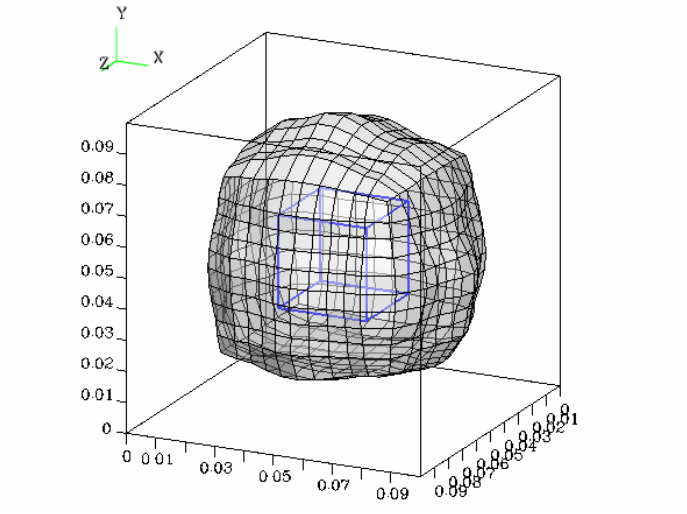

(a)

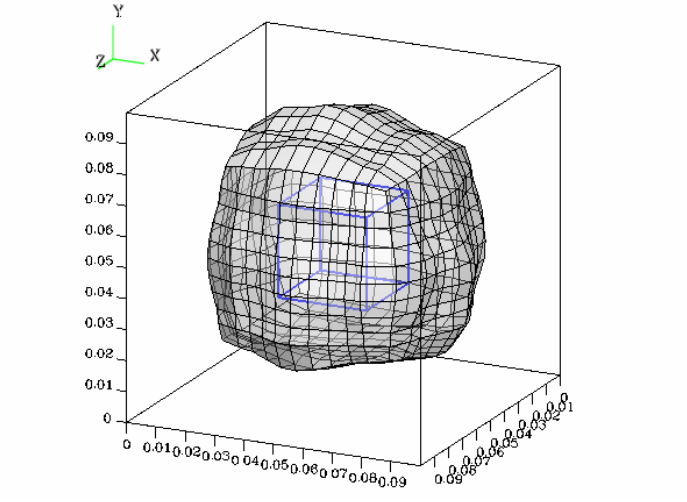

(b)

Figure 9: The estimated interfacial enclosures using (a) $\sigma = 0.504$ and (b) $\sigma = 0.84$ and type A initial guess in case 2.

From the above three numerical test cases, it is learned that the SDM can be applied successfully in estimating unknown interfacial enclosure in a multiple region domain with an internal cavity. Reliable estimations can also be obtained when measurement errors are considered.

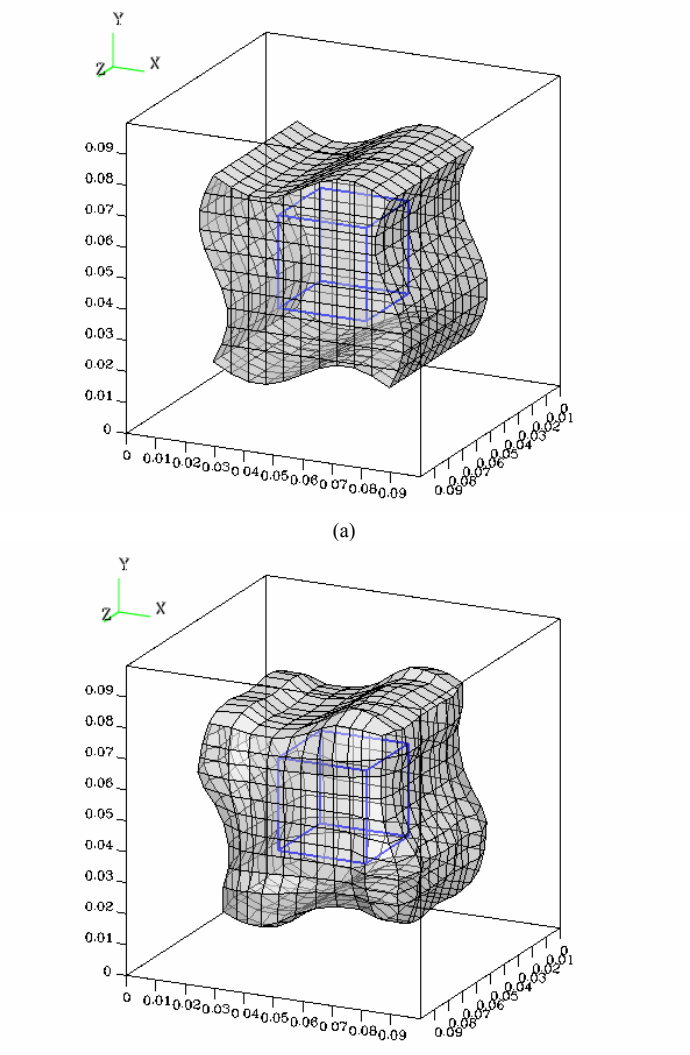

Figure 10: The (a) exact and (b) estimated interfacial enclosures using type A initial guess and $\sigma = 0.0$ in case 3.

10 Conclusions

The steepest descent method (SDM) together with the commercial code CFD-ACE+ were successfully applied for the solution of the three-dimensional thermal

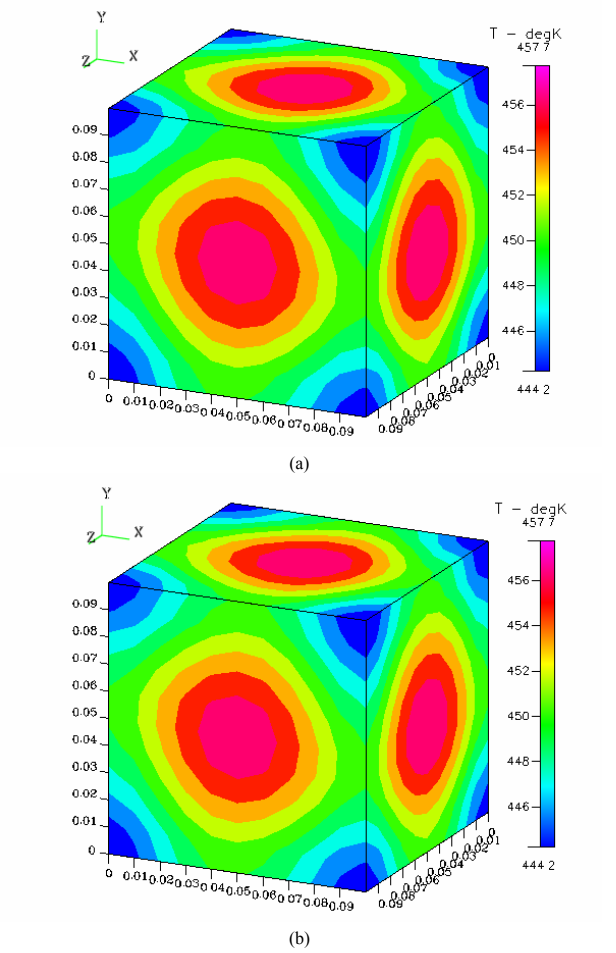

Figure 11: The (a) measured and (b) estimated surface temperatures on S_o using σ = 0.0 in case 3.

tomography problem to estimate the unknown interfacial enclosure in a multiple region domain with an internal cavity by utilizing surface temperature readings. Three test cases involving different shape of interfacial enclosures, different shape of initial guess interfacial enclosures and different measurement errors were considered. The results show that the SDM does not require an accurate initial guesses of the unknown quantities, does not need any extra assumptions, does not need very long CPU time on Intel®Pentium D CPU 2.8 GHz PC and is not sensitive to the measurement errors when performing the thermal tomography calculations.

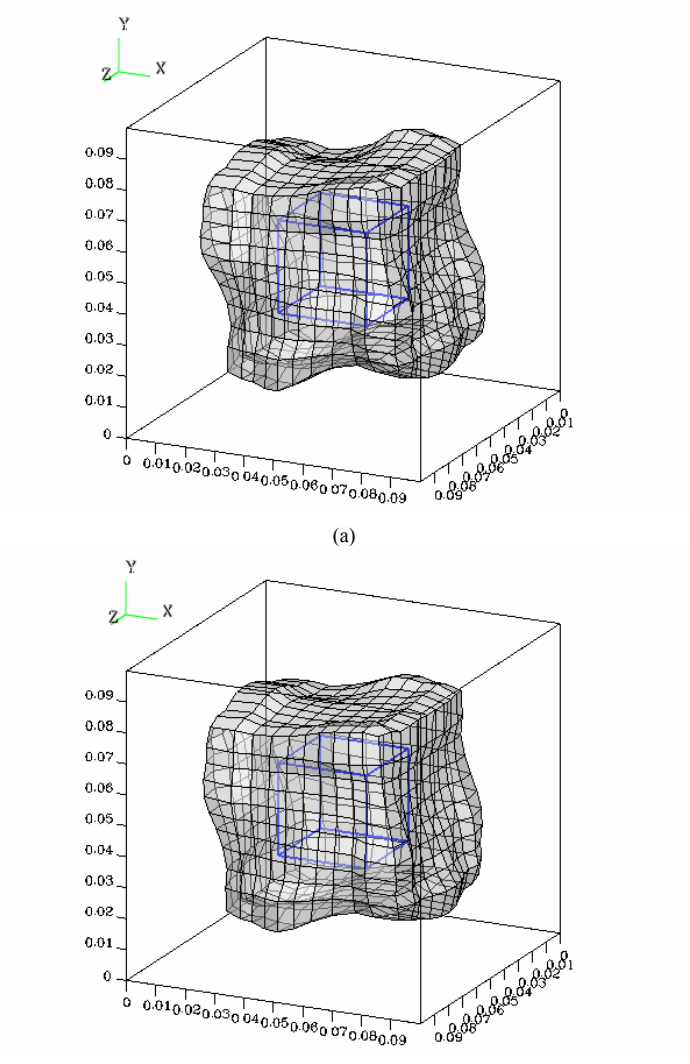

Figure 12: The estimated interfacial enclosures using (a) $\sigma = 0.405$ and (b) $\sigma = 0.675$ and type A initial guess in case 3.

Acknowledgement: This work was supported in part through the National Science Council, R. O. C., Grant number, NSC-96-2221-E-006-332-MY3.

References

Alifanov, O. M. (1994): *Inverse heat transfer problems*. Springer-Verlag, Berlin Heidelberg.

Aoki, S., Amaya, K., Urago, M., Nakayama, A. (2005): Fast Multipole Boundary Element Analysis of Corrosion Problems. *CMES: Computer Modeling in Engineering & Sciences*, vol. 6, no. 2, pp. 123–132.

Burczynski, T., Beluch, W., Dlugosz, A., Kus, W., Nowakowski, M., Orantek, P. (2002): Evolutionary Computation in Optimization and Identification, *Comput. Assist. Mech. Eng. Sci.,* Vol. 9, pp. 3–20.

Burczinski,T., Kane, J. H., Balakrishna, C. (1995): Shape Design Sensitivity Analysis via Material Derivative-Adjoint Variable Technique for 3D and 2D Curved Boundary Elements, *Int. J. Numer. Meth. Eng.,* Vol. 38, pp. 2839–2866.

CFD-ACE+ user's manual, ESI-CFD Inc. (2005).

Chen, W. L., Yang, Y. C. (2009): Inverse estimation for the unknown frost geometry on the external wall of a forced-convection pipe, *Energy Conversion and Management*, Vol. 50, pp.1457–1464.

Chen, W. L., Yang, Y. C. and Lee, H. L. (2009): Three-Dimensional Pipe Fouling Layer Estimation by Using Conjugate Gradient Inverse Method, *Numerical Heat Transfer, Part A*, Vol. 55, pp. 845–865.

Cheng, C. H., Wu, C. Y. (2000): An Approach Combining Body-Fitted Grid Generation and Conjugate Gradient Methods for Shape Design in Heat Conduction Problems, *Numer. Heat Transfer B,* Vol. 37, pp. 69–83.

Dems, K., Mroz, Z. (1987): Variational approach to sensitivity analysis in thermoelasticity, *J. Thermal Stresses,* Vol. 10, pp.283–306.

Dems, K., Mroz , Z. (1998): Sensitivity analysis and optimal design of external boundaries and interfaces for heat conduction systems, *J. Thermal Stress,* Vol. 21, No. 3-4, pp. 461-488**.**

Divo, E., Kassab, A. J., Rodriguez, F. (2004): An Efficient Singular Superposition Technique for Cavity Detection and Shape Optimization, *Numerical Heat Transfer;* Part B, Vol. 46, pp. 1-30.

Forth, S., Staroselsky, A. (2005): A Hybrid FEM/BEM Approach for Designing an Aircraft Engine Structural Health Monitoring. *CMES: Computer Modeling in Engineering & Sciences*, vol. 9, no. 3, pp. 287–298.

Hsieh, C. K., Choi, C. Y., Liu, K. M. (1989): A Domain Extension Method for Quantitative Detection of Cavities by Infrared Scanning, *J. Nodes. Eval.,* Vol. 8, pp. 195-211.

Huang, C. H., Chaing, M. T. (2008): A Transient Three-Dimensional Inverse Geometry Problem in Estimating the Space and Time-Dependent Irregular Boundary Shapes, *Int. J. Heat and Mass Transfer.* Vol. 51, No. 21-22, pp. 5238–5246.

Huang, C. H., Chao, B. H. (1997): An Inverse Geometry Problem in Identifying Irregular Boundary Configurations, *Int. J. Heat and Mass Transfer*, Vol. 40, pp. 2045-2053.

Huang, C. H., Chen, C. A. (2008): The Shape Identification Problem in Estimating the Geometry of A Three-Dimensional Irregular Internal Cavity, *CMES: Computer Modeling in Engineering & Sciences*, Vol. 36, no. 1, pp. 1–21.

Huang, C. H., Chiang, C. C., Chen, H. M. (1998): Shape Identification Problem in Estimating the Geometry of Multiple Cavities, *AIAA, J. Thermophysics and Heat Transfer*, Vol. 12, pp. 270-277.

Huang, C. H., Hsiung, T. Y. (1999): An Inverse Design Problem of Estimating Optimal Shape of Cooling Passages in Turbine Blades, *Int. J. Heat and Mass Transfer*, Vol. 42, No. 23, pp. 4307-4319.

Huang, C. H., Tsai, C. C. (1998): A Transient Inverse Two-Dimensional Geometry Problem in Estimating Time-Dependent Irregular Boundary Configurations, *Int. J. Heat and Mass Transfer*, Vol. 41, pp. 1707-1718.

IMSL Library Edition 10.0, (1987): User's Manual: Math Library Version 1.0, IMSL, Houston, TX.

Jeong, C.; Kallivokas, L. F. (2008): Inverse Scatterer Reconstruction in a Half-plane Using Surficial SH Line Sources. *CMES: Computer Modeling in Engineering & Sciences*, 35: 49-71.

Kassab, A. J., Hsieh, C. K. (1987): Application and Infrared Scanners and Inverse Heat Conduction Methods to Infrared Computerized Axial Tomography, *Rev. Sci. Inst.,* Vol. 58, pp. 89-95.

Kwag, D. S., Park, I. S., Kim, W. S. (2004): Inverse Geometry Problem of Estimating the Phase Front Motion of Ice in A Thermal Storage System, *Inverse Problems in Science and Engineering*, Vol. 12, No. 1, pp. 1–15.

Liu, C. S., Chang, C. W., Chiang, C. Y. (2008): A regularized integral equation method for the inverse geometry heat conduction problem, *International Journal of Heat and Mass Transfer*, Vol. 51, pp. 5380–5388.

Mera, N. S., Elliott, L., Ingham, D. B. (2006): The Detection of Super-elliptical Inclusions in Infrared Computerised Axial Tomography, *CMES: Computer Modeling in Engineering & Sciences*, Vol. 6, No. 2, pp. 123-132.